

Protection effect of a SiO₂ layer in Al_{0.85}Ga_{0.15}As wet oxidation*

Zhou Wenfei(周文飞)^{1,2,†}, Ye Xiaoling(叶小玲)¹, Xu Bo(徐波)¹, Zhang Shizhu(张世著)¹, and Wang Zhanguo(王占国)¹

¹Key Laboratory of Semiconductor Materials Science, Institute of Semiconductors, Chinese Academy of Sciences, Beijing 100083, China

²Department of Physics, Tsinghua University, Beijing 100084, China

Abstract: The Al_{0.85}Ga_{0.15}As layers buried below the GaAs core layer with and without the SiO₂ layer were successfully oxidized in a wet ambient environment. The experimental results show that the SiO₂ layer has little impact on the lateral-wet-oxidation rate of the Al_{0.85}Ga_{0.15}As layer. The contrast of the SEM image of the oxidized regions and the absence of As-related Raman peaks for samples with the SiO₂ layer arise from the removal of As ingredients with the largest atomic number, which leads to improvements in the thermal stability of the oxidized layer. The PL intensities of samples with the SiO₂ layer are much stronger than those without the SiO₂ layer. The PL emission peak is almost unshifted with a slight broadening under the protection of the SiO₂ layer. This is attributed to the SiO₂ layer preventing oxidation damage to the GaAs capping layer.

Key words: lateral wet oxidation; SiO₂ protection layer; InAs QDs

DOI: 10.1088/1674-4926/33/10/102002

EEACC: 2520; 2550

1. Introduction

The lateral wet oxidation of the buried Al_xGa_{1-x}As layer has been widely used in the fabrication of various optical devices due to its optical mode and current confinement. For example, in vertical cavity surface emitting lasers (VCSELs), single-photon emitters, metal-insulator-semiconductor field effect transistors (MIS-FETs) and electrically pumped photonic crystal lasers^[1-7]. The oxidation rate increases with increasing oxidation temperature and layer thickness, whereas there is a significant reduction with decreasing Al content^[8,9]. In order to control the oxidation rate precisely, it is appropriate to use the buried Al_xGa_{1-x}As layer with a low Al content ($x < 0.90$).

Semiconductor quantum dots (QDs) exhibit discrete optical transitions with ultra-narrow linewidths, and they are applied as an emitter in various nanoscale photonic devices. Up to now, a number of works on devices with an active region made up of single or multiple In(Ga)As QDs sheets in a GaAs matrix have been reported by various groups^[5-7,10,11]. Generally, the GaAs core layer with QD sheets is grown epitaxially on top of the buried Al_xGa_{1-x}As layer. In the process of lateral wet oxidation, it has been reported that oxidation damage to the GaAs capping layer is induced at about 450 °C^[12]. Because the GaAs capping layer is extremely thin, even a small amount of oxidation would degrade the optical characteristics of the QD ensemble^[13]. Furthermore, an additional annealing is needed for removing the remaining oxidation product, As, in the oxidized region, improving the thermal stability of the oxidized layer^[14]. It is imperative to find a way in which the lateral wet oxidation of the buried Al_xGa_{1-x}As layer has little impact on the GaAs capping layer, and the remaining reaction products

are removed at the same time. In this paper, we present an effective method to protect the GaAs capping layer and eliminate the remaining reaction product (As) in a wet oxidation ambient environment.

2. Experimental details

The sample structure for the oxidation experiments is shown in Fig. 1. We used an n-type GaAs-based heterostructure: a single layer of high density InAs QDs was grown by molecular beam epitaxy (MBE) at the center of a 180 nm GaAs membrane. The membrane was grown on top of a 420 nm Al_{0.85}Ga_{0.15}As sacrificial layer. The 160 nm SiO₂ layer was deposited by plasma enhanced chemical vapor deposition (PECVD) on the top of the GaAs membrane. Circular mesas with a diameter of 50 μm were defined by the use of photoresist, reactive ion etching and inductively coupled plasma etching. After photoresist, the patterns were transferred

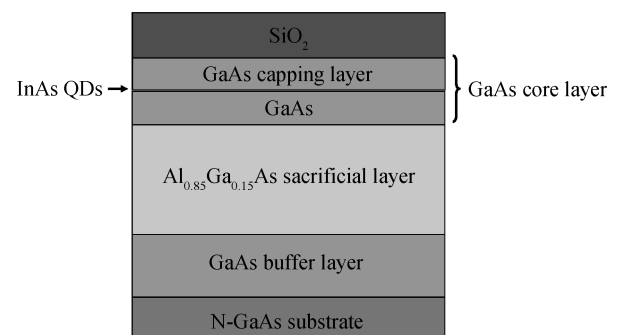


Fig. 1. Schematic of the sample structure for the oxidation experiments.

* Project supported by the National Research Project of China (Nos. 60990315, 60625402, 61161130527).

† Corresponding author. Email: wfzhou@semi.ac.cn

Received 21 March 2012, revised manuscript received 27 April 2012

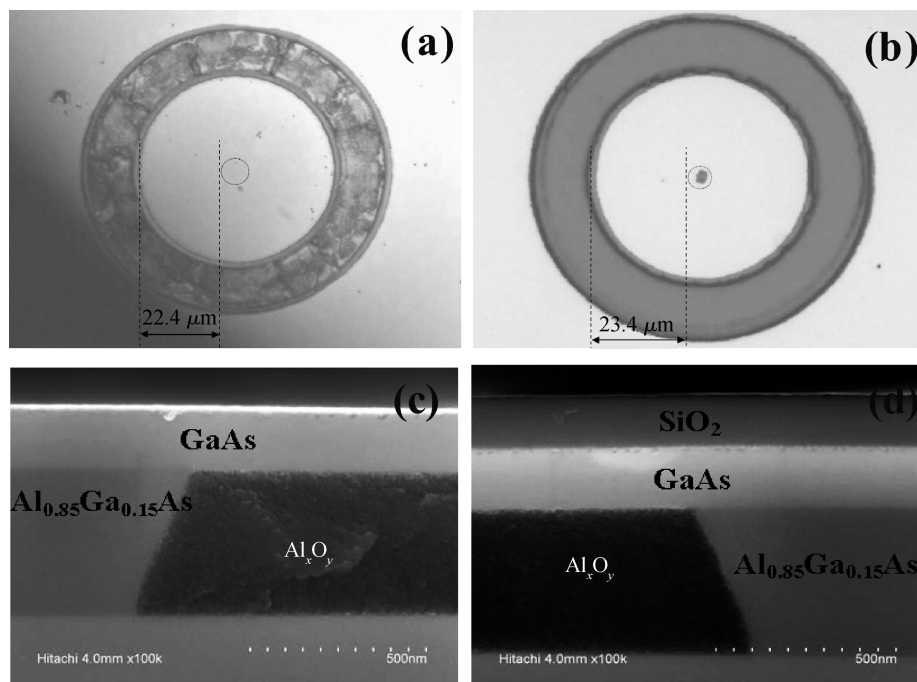


Fig. 2. (a) and (b) plan-view optical microscope and (c) and (d) cross-sectional FE-SEM images of the samples after the lateral wet oxidation. (a) and (c) are without the SiO_2 layer; (b) and (d) are with the SiO_2 layer.

from the resist to the SiO_2 layer using reactive ion etching. Finally, mesas patterns were transferred from the SiO_2 layer by chlorine-based gases inductively coupled plasma etching, and the process was stopped until the buried $\text{Al}_x\text{Ga}_{1-x}\text{As}$ layer was etched completely. For a comparison, a circular mesas without the SiO_2 layer was also fabricated.

Prior to wet oxidation, samples were heated to the reaction temperature in dry nitrogen. The oxidation was carried out in a quartz-tube furnace at 550°C in an H_2O vapor atmosphere, which was created by bubbling N_2 carrier gas at 1.5 L/min through the water bubbler at 90°C . Oxidation proceeds laterally in the $\text{Al}_{0.85}\text{Ga}_{0.15}\text{As}$ layer beneath the GaAs core layer. The samples were oxidized for 2.5 h. The reaction was terminated by switching to a dry nitrogen flow. After the oxidation, the $\text{Al}_{0.85}\text{Ga}_{0.15}\text{As}$ ($n \approx 3.4$) is converted into a stable native oxide and its refractive index is changed ($n \approx 1.6$). Therefore, when we look at the surface using an optical microscope, the color is different between oxidized and unoxidized parts.

The morphologies of the oxidized samples were observed by optical microscope and field emission scanning electron microscopy (FE-SEM). Photoluminescence measurements were performed using the 532 nm solid state laser as the excitation source and the signal was collected using the Fourier Transformed Infrared Spectrometer with an In(Ga)As detector. Micro-Raman spectra were measured using an excitation wavelength of 514.5 nm line of an Ar^+ laser.

3. Results and discussion

The plan-view optical microscope morphologies of the oxidized samples are shown in Figs. 2(a) and 2(b). We can see that the $\text{Al}_{0.85}\text{Ga}_{0.15}\text{As}$ layer is laterally oxidized from a mesas edge in the steam environment. The oxidation lengths are about $22.4\ \mu\text{m}$ and $23.4\ \mu\text{m}$, and the oxidation rates are

about $9.0\ \mu\text{m/h}$ and $9.3\ \mu\text{m/h}$, respectively. That is to say, the SiO_2 layer has little impact on the lateral-wet-oxidation-rate of the $\text{Al}_{0.85}\text{Ga}_{0.15}\text{As}$ layer. The cross-sectional FE-SEM morphologies of the oxidized samples are shown in Figs. 2(c) and 2(d). It can be found that the oxidized and unoxidized regions exhibit different colors, and the oxidized region is marked as Al_xO_y . It can be also observed that the color of the oxidized region with the SiO_2 layer is much darker than that without the SiO_2 layer, but there are almost the same colors in other corresponding regions.

Figures 3(a) and 3(b) display Raman spectra for samples without the SiO_2 layer. Raman spectrum of the as-prepared samples are shown in Fig. 3(a). The peaks at 293 and $269\ \text{cm}^{-1}$ are separately attributed to longitudinal optical GaAs (LO-GaAs) and transverse optical GaAs (TO-GaAs). The weak peak intensities at about 400 and $362\ \text{cm}^{-1}$ are AlAs-related peaks^[15, 16]. The curves I, II, III and IV indicate Raman spectra for the thermally oxidized mesas, and the distances of the measuring position to the center of the mesas are $22.5\ \mu\text{m}$ (I), $15\ \mu\text{m}$ (II), $7.5\ \mu\text{m}$ (III), $0\ \mu\text{m}$ (IV), respectively. It can be seen that crystalline As peaks appear at 198 and $257\ \text{cm}^{-1}$ besides the GaAs-related peaks after the wet oxidation^[15, 16]. The signal intensities of the As-related peaks grow stronger as the distance between the measuring positions to the center of the mesas decreases. Figures 3(c) and 3(d) indicate Raman spectra for samples with the SiO_2 layer. The GaAs-related and AlAs-related peaks are the same as those without the SiO_2 layer for as-prepared samples. After wet oxidation, in all Raman spectra, crystalline As-related peaks at 198 and $257\ \text{cm}^{-1}$ are not detectable. Because the band gap ($5.2\ \text{eV}$) of the SiO_2 is much larger than the energy ($2.4\ \text{eV}$) of the Ar^+ laser beam, the incident laser power is little affected by the SiO_2 layer. It can be concluded that the absence of As-related peaks attributes to the inexistence of As ingredients in the oxidized region.

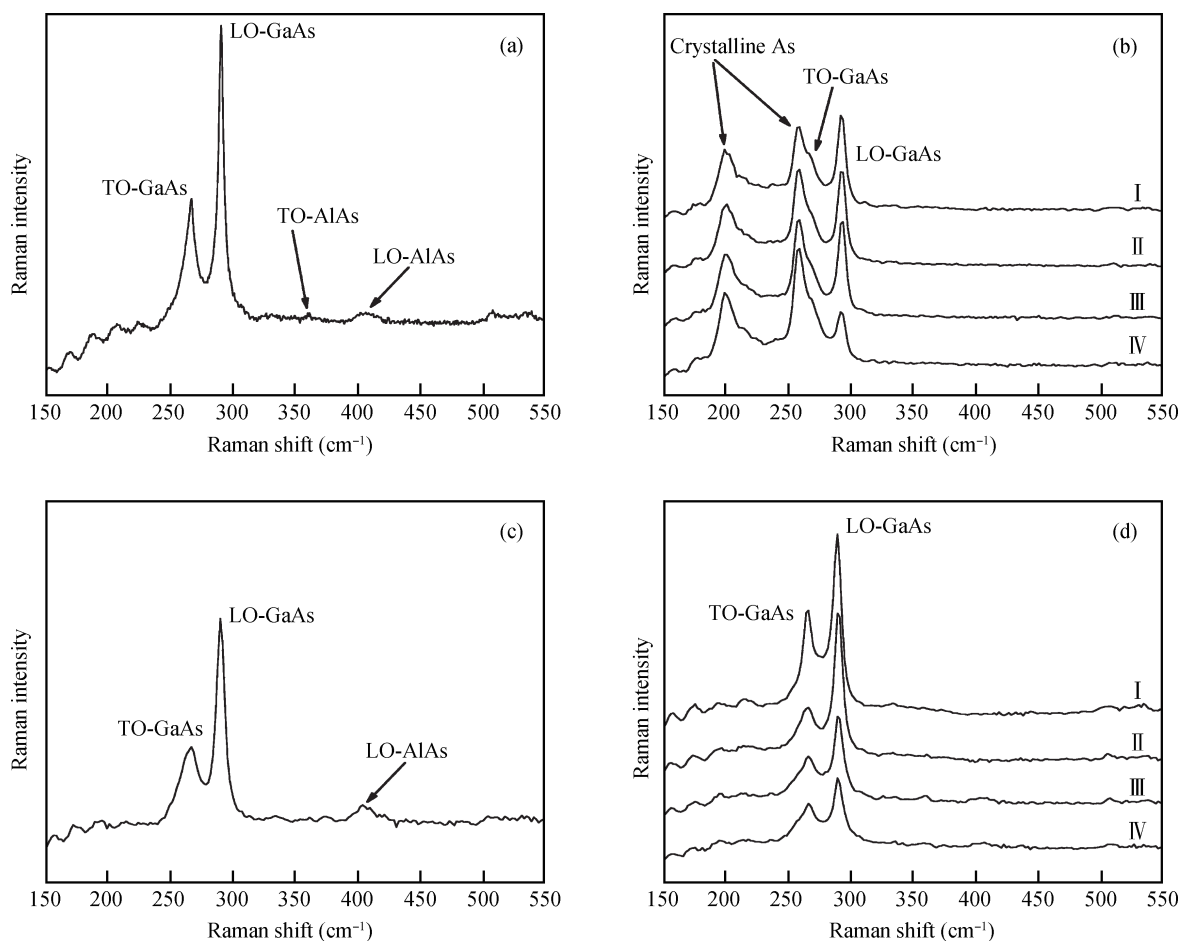


Fig. 3. Raman spectra ((a) and (b)) without and ((c) and (d)) with the SiO₂ layer. (a) and (c) indicate Raman spectrum of as-prepared samples, and Raman spectrum of the oxidized samples are shown in (b) and (d). The distance of the measuring position to the center of the mesas are 22.5 μm (I), 15 μm (II), 7.5 μm (III), 0 μm (IV), respectively.

In the process of the wet oxidation, the Al_{0.85}Ga_{0.15}As layer may change to As, As₂O₃ and Al₂O₃^[14–16]. The oxidation layer is a porous structure, providing a natural channel for the escape of volatile reaction products such as As and As₂O₃. However, when the wet oxidation proceeds towards the center of the mesas, the escape of volatile products will be increasingly difficult. Therefore, there are increasingly rising intensities of crystalline As peaks at 198 and 257 cm⁻¹.

It is reported that the As atoms can fill Ga vacant (V_{Ga}) sites forming arsenic antisites (As_{Ga})^[17–19]. Day *et al.*^[20] also demonstrated that As_{Ga} defects can be created and their concentration can be enhanced by high temperature annealing due to V_{Ga} defects arising from the out-diffusion of Ga atoms into the dielectric film. In our experiment, the V_{Ga} defects can also be created near the SiO₂ layer/GaAs interface during the heat treatment. Additionally, because GaAs has a much larger thermal expansion coefficient^[21] ($6.03 \times 10^{-6} \text{ }^\circ\text{C}^{-1}$) than SiO₂^[22] ($0.52 \times 10^{-6} \text{ }^\circ\text{C}^{-1}$), a compressive stress in the GaAs layer is created during the wet oxidation, which helps V_{Ga} defects diffuse rapidly from the sample surface towards the depth over several microns and distribute in a relatively uniform concentration^[23]. At the same time, As ingredients in the oxidized region can diffuse into the GaAs layer by a concentration gradient. Therefore, it is possible that the As atoms can fill the V_{Ga} sites forming As_{Ga}. Along with the constant consumption

of As atoms in the GaAs layer to fill V_{Ga} sites, As ingredients can diffuse constantly into the GaAs layer, and the concentration of As ingredients in the oxidized region decreases drastically. When the concentration is under the detecting limit, the As-related peaks are absent in Raman spectra.

For samples without the SiO₂ layer, annealing can result in the loss of As atoms from the sample surface, hence, generating As vacancies (V_{As})^[24, 25]. Additionally, surface oxidation of the GaAs capping layer can be induced^[12] due to the wet oxidation at 550 °C. Therefore, the surface oxide layer can prevent the further out-diffusion of As atoms. It can be concluded that there exist a limited number of As vacancies in the GaAs layer. In other words, it is possible that only a minority of As atoms in the oxidized region can diffuse into the GaAs layer to fill As vacancy sites. Therefore, a majority of As ingredients reside in the oxidized region, which leads to the appearance of crystalline As peaks in the Raman spectra.

It is known that the secondary electron image contrast of SEM images results from surface irregularities and different compositions^[26, 27]. In the experiment, the samples have smooth cross-sections, so the contrast of the oxidized regions with and without the SiO₂ layer in Fig. 2 arises from the composition contrast. Essentially, the composition contrast attributes to the differences of the average atomic number in different regions^[27]. It is reported that the secondary electron

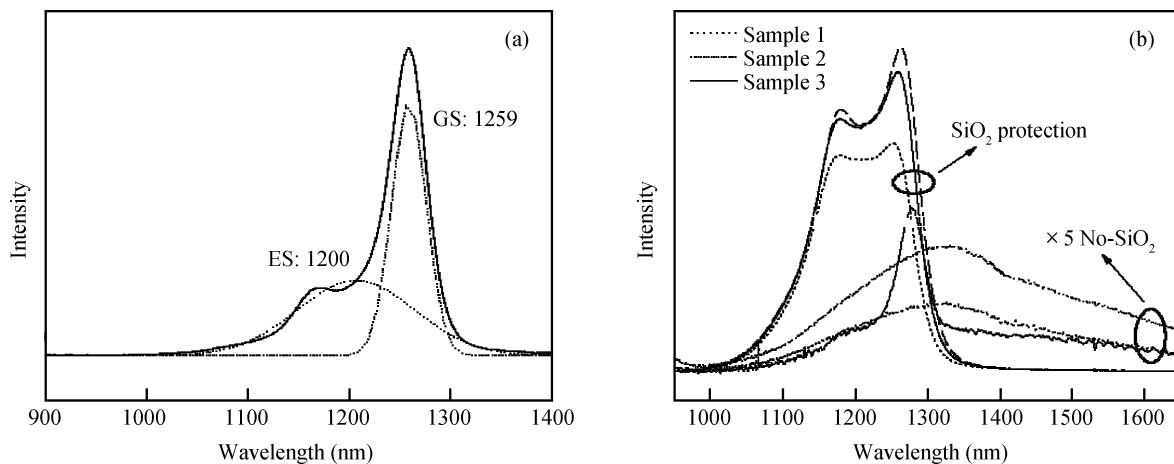


Fig. 4. (a) PL spectrum of the as-grown QD ensemble at room temperature. GS indicates the ground state emission and ES the excited state. (b) PL spectra of the QD ensemble at room temperature after the wet oxidation.

yield increases with the increase of the average atomic number, and the larger the average atomic number is, the brighter the corresponding region is^[28]. The atomic numbers of O, Al, Ga and As are 8, 13, 31 and 33 respectively. When As ingredients with the largest atomic number are removed from the oxidized region with the SiO₂ layer, the average atomic number decreases. So it leads to the composition contrast in the oxidized regions with and without the SiO₂ layer.

Figure 4(a) shows the photoluminescence (PL) spectrum for an as-grown QD ensemble at room temperature. The spectral peak positions of the ground state and the excited state are around 1260 nm and 1200 nm, respectively. The full width at half maximum (FWHM) of the ground state peak is about 46 nm. After the wet oxidation, the PL spectra of the QD ensemble at room temperature are displayed in Fig. 4(b). In order to explain the protection effect of the SiO₂ layer convincingly, three groups of samples are used, which are indicated by dotted (sample 1), dashed (sample 2) and solid (sample 3) lines, respectively. It can be clearly observed that the PL intensity of samples with the SiO₂ layer is much stronger than those without the SiO₂ layer. The emission peak and the FWHM are nearly unchanged under the protection of the SiO₂ layer. However, for no-SiO₂ samples, the wet oxidation leads to a redshift and a broadening of optical emission from QDs.

Thermal annealing has been widely performed to improve the quality of QDs^[29–31]. The interdiffusion of the In and Ga atoms at the interface between the QD and the GaAs barrier can result in an emission blueshift, a peak narrowing, and, in some cases, a decrease in PL intensity. It is reported that annealing temperatures below 600 °C have little impact on the optical properties of the QD ensemble. Therefore, annealing is usually carried out above 600 °C in an argon or nitrogen ambient. Under the protection of an inert atmosphere, the GaAs capping layer is almost thermally unoxidized.

In the experiment, the oxidation is carried out at 550 °C in a wet ambient environment, as it is believed that the annealing effect has little impact on the optical properties of the QDs ensemble. In the process of the lateral wet oxidation without an inert atmosphere, surface oxidation damage to the GaAs capping layer is induced at about 450 °C^[12], which may cause strain relaxation. It is reported that strain relaxation can give

rise to a change in both conduction band edge and valence band edge^[32, 33]. So the energy band gap of InAs QDs may be reduced due to strain relaxation, which results in a redshift of the PL peak position. Additionally, for no-SiO₂ samples, the wet oxidation can induce a large number of nonradiative recombination centers at the surface of the GaAs capping layer. So the reduced emission intensity is due to the strong nonradiative recombination at the surface of the GaAs capping layer. The lifetime of carriers in InAs QDs is shortened due to nonradiative recombination at the surface, which leads to a much broader PL linewidth. However, the SiO₂ layer on top of the GaAs capping layer can prevent the oxidation of the GaAs capping layer. Therefore, the optical properties of the QDs ensemble with the SiO₂ layer are similar to those of the unannealed samples.

4. Conclusion

In summary, the SiO₂ protection for the GaAs capping layer in the wet oxidation ambient environment has been studied using SEM, Raman and PL spectroscopy measurements. The experimental results show that the SiO₂ layer has little impact on the lateral-wet-oxidation rate of the Al_{0.85}Ga_{0.15}As layer. The contrast of the SEM image of the oxidized regions and the absence of As-related Raman peaks for samples with the SiO₂ layer arise from the removal of As ingredients with the largest atomic number, which leads to improve the thermal stability of the oxidized layer. The PL intensity with the SiO₂ layer is much stronger than that without the SiO₂ layer. The PL emission peak is almost unshifted with a slight broadening under the protection of the SiO₂ layer. They are attributed to the SiO₂ layer preventing the oxidation damage to the GaAs capping layer. Our results are of vital importance to improve the potential performance of the nanodevices.

Acknowledgements

The authors are sincerely grateful to Mr. Hu Chuanxian and Dr. Fan Zhongchao at the Engineering Research Center of Semiconductor Integrated Technology, Institute of Semiconductors, Chinese Academy of Sciences, and to Mrs. Liang

Ping, for their help and encouragement throughout the course of this work.

References

- [1] Huffaker D L, Deppe D G, Shin J. Threshold characteristics of planar and index-guided microcavity lasers. *Appl Phys Lett*, 1995, 67: 4
- [2] Hayashi Y, Mukaiharu T, Hatori N, et al. Record low-threshold index-guided InGaAs/GaAlAs vertical-cavity surface emitting laser with a native oxide confinement structure. *Electron Lett*, 1995, 31: 560
- [3] Fiore A, Chen, J X, Ilegems M. Scaling quantum-dot light-emitting diodes to submicrometer sizes. *Appl Phys Lett*, 2002, 81: 1756
- [4] Chen E I, Holonyak N, Maranowski S A. Al_xGa_{1-x}As–GaAs metal–oxide–semiconductor field-effect transistors formed by lateral water-vapor oxidation of AlAs. *Appl Phys Lett*, 1995, 66: 2688
- [5] Chen L, Towe E. Design of high-*Q* microcavities for proposed two dimensional electrically pumped photonic crystal lasers. *IEEE J Sel Top Quant*, 2006, 12: 117
- [6] Kim Y K, Elarde V C, Long C M, et al. Electrically injected InGaAs/GaAs photonic crystal embrane light emitting microcavity with spatially localized gain. *J Appl Phys*, 2008, 104: 123103
- [7] Chakravarty S, Bhattacharya P, Topol'ančik J, et al. Electrically injected quantum dot photonic crystal microcavity light emitters and microcavity arrays. *J Phys D: Appl Phys*, 2007, 40: 2683
- [8] Langenfelder T, Schroder S, Grothe H. Lateral oxidation of buried Al_xGa_{1-x}As layers in a wet ambient. *J Appl Phys*, 2007, 82: 3548
- [9] Kim J H, Lim D H, Kim K S, et al. Lateral wet oxidation of Al_xGa_{1-x}As–GaAs depending on its structures. *Appl Phys Lett*, 1996, 69: 3357
- [10] Nomura M, Iwamoto S, Nishioka M, et al. Highly efficient optical pumping of photonic crystal nanocavity lasers using cavity resonant excitation. *Appl Phys Lett*, 2006, 89: 161111
- [11] Nomura M, Iwamoto S, Nishioka M, et al. Cavity resonant excitation of InGaAs quantum dots in photonic crystal nanocavities. *Jpn J Appl Phys*, 2006, 45: 6091
- [12] Takamori T, Takemasa K, Kamijoh T. Interface structure of selectively oxidized AlAs/GaAs. *Appl Phys Lett*, 1996, 69: 659
- [13] Tanaka Y, Sugimoto Y, Ikeda N, et al. Fabrication and characterization of AlGaAs-based photonic crystal slab waveguides by precisely controlled self-aligned selective-oxidation process. *Jpn J Appl Phys*, 2003, 42: 7331
- [14] Jia H Q, Chen H, Wang W C, et al. Improved thermal stability of wet-oxidized AlAs. *Appl Phys Lett*, 2002, 80: 974
- [15] Haisler V A, Hopfer F, Sellin R L, et al. Micro-Raman studies of vertical-cavity surface-emitting lasers with Al_xO_y–GaAs distributed Bragg reflectors. *Appl Phys Lett*, 2002, 81: 2544
- [16] Carol I H, Ashby J P, Sullivan P P, et al. Wet oxidation of Al_xGa_{1-x}As: temporal evolution of composition and microstructure and the implications for metal–insulator–semiconductor applications. *Appl Phys Lett*, 1997, 70: 2443
- [17] Reddy C V, Fung S, Beling C D. Nature of the bulk defects in GaAs through high-temperature quenching studies. *Phys Rev B*, 1996, 54: 11290
- [18] Kaniewska M, Engström O, Barcz A, et al. Deep levels induced by InAs/GaAs quantum dots. *Mater Sci Eng C*, 2006, 26: 871
- [19] Bourgoin J C, Hammadi H, Stellmacher M, et al. As antisite incorporation in epitaxial growth of GaAs. *Physica B*, 1999, 273: 725
- [20] Day D S, Oberster J D, Drummond T J, et al. Electron traps created by high temperature annealing in MBE n-GaAs. *J Electron Mater*, 1981, 10: 445
- [21] Brozel M R, Stillman G E. Properties of GaAs, *Emis Data Review Series*. London, INSPEC, IEE, 1996
- [22] Lide D R. CRC handbook of chemistry and physics. 73rd. Cleveland, OH, Chemical Rubber Publishing Company, 1993
- [23] Pepin A, Vieu C, Schneider M, et al. Evidence of stress dependence in SiO₂/Si₃N₄ encapsulation-based layer disordering of GaAs/AlGaAs quantum well heterostructures. *J Vac Sci Technol B*, 1997, 15: 142
- [24] Bhattacharyya D, Helmy A S, Bryce A C, et al. Selective control of self-organized In_{0.5}Ga_{0.5}As–GaAs quantum dot properties: quantum dot intermixing. *J Appl Phys*, 2000, 88: 4619
- [25] Reddy C V, Fung S, Beling C D. Nature of the bulk defects in GaAs through high-temperature quenching studies. *Phys Rev B*, 1996, 54: 11290
- [26] Liu A S, Shao B L, An S, et al. Applications of secondary electron composition contrast imaging method in microstructure studies on heterojunction semiconductor devices and materials. *Chinese J Rare Metals*, 1998, 22(6): 980601
- [27] Wang X Q, Hong Y, Zhang A H, et al. SEM secondary electron imaging in the V-doped SiC growth by PVT. *Semicond Tech*, 2010, 35: 317
- [28] Xu J, Chen W X, Zhang H Z. Composition contrast in high resolution secondary electron image. *J Chin Electr Microsc Soc*, 1997, 16(1): 1
- [29] Guimard D, Ishida M, Bordel D, et al. Ground state lasing at 1.30 μm from InAs/GaAs quantum dot lasers grown by metal–organic chemical vapor deposition. *Nanotechnology*, 2010, 21: 105604
- [30] Liang S, Zhu H L, Ye X L, et al. Annealing behaviors of long-wavelength InAs/GaAs quantum dots with different growth procedures by metalorganic chemical vapor deposition. *J Cryst Growth*, 2009, 311: 2281
- [31] Malik S, Roberts C, Murraya R, et al. Tuning self-assembled InAs quantum dots by rapid thermal annealing. *Appl Phys Lett*, 1997, 71: 1987
- [32] Liang B L, Wang Z M, Mazur Y I, et al. Correlation between surface and buried InAs quantum dots. *Appl Phys Lett*, 2006, 89: 043125
- [33] Miao Z L, Zhang Y W, Chua S J, et al. Optical properties of InAs/GaAs surface quantum dots. *Appl Phys Lett*, 2005, 86: 031914